
PHYS 305 FINAL PROJECT

Philip N. Klaassen
The University of Arizona

ABSTRACT

This investigation aims to reproduce the results found in Koen et. al. (2012) [1], using a smaller number of particles and larger time step. We show that accurate energy peaks and stabilization results are achievable with ten times fewer particles, and a coarser time scale. However, as a consequence of smaller electron number density a larger amount of high frequency noise in the electric field was recorded. We find this noise can be solved by decreasing spatial resolution, but resolution does not allow distinguishable dispersion relations to be found. In addition we were unable to adequately distinguish the differences in wave modes due to plasma parameters as described by Koen et al. While our changes allowed much faster computation, the degradation of the simulation results ultimately rule out these time-saving changes and justify the original choice of particle number and time step.

1 Introduction

Plasmas are common in many areas of research, including space weather, Aurora, and the Interplanetary Medium. There are also many practical applications to studying plasmas, for example, electrostatic waves found in earth's magnetosphere may be responsible for certain forms of electrostatic noise, and understanding these sources is important for many forms of communication.

Three of the possible electrostatic wave modes found in plasmas are the electron acoustic, electron plasma, and beam-driven wave modes. Beam-driven instabilities are excited by a species of streaming electrons at a higher relative velocity that interact with another slower species of electron. Electron beams allow us to introduce more kinetic energy into a system in a physical way, and they are also useful to model many physical situations in various space plasmas. Electron acoustic wave modes survive for a non-depreciable time in plasmas with a hot and cold component[2]. We designed our simulation based on the procedures described in Brelsall&Langdon (1991)[3], as did Koen et. al. We used the same physical plasma parameters as described by Koen et. al. but changed the particle number and time step.

Simulations are a practical way to investigate plasmas, of these Particle in Cell, PIC, simulations are common on small spatial scales due to their accuracy and computational expense relative to other methods such as Magneto-Hydrodynamic simulations. The PIC philosophy is grounded in the impracticality of computing particle-on-particle interactions for each particle in a plasma. Instead, a PIC style simulation places particles in a spatial grid, accumulates charges on the spatial grid to derive a charge distribution which is known at the grid points. Then using Maxwell equations we are able to find the electric and magnetic fields at the grid points. Lastly, the fields are interpolated to the particle positions from the grid points and used to update the particle positions and velocities. We used a 1-D PIC simulation.

2 Theory

The Plasma of interest in this study was a three-species unmagnetized plasma consisting of hot, cold, and beam electrons. There was also an immobile species of background ions, meant only to ensure a net charge of zero. For each species, j the Debye Length is

$$\lambda_j = \left(\frac{\epsilon_0 k_B T_j}{n_j e^2} \right)^{\frac{1}{2}} \quad (1)$$

and the plasma frequency is

$$\omega_j = \left(\frac{n_j e^2}{m_e \epsilon_0} \right)^{\frac{1}{2}}, \quad (2)$$

where n_j is the number density of the j th species of electron. From Koen et. al. the dispersion relation for Electron Plasma Waves is

$$\omega = (\omega_c^2(1 + 3(k\lambda_c)^2) + \omega_h^2(1 + 3(k\lambda_h)^2))^{\frac{1}{2}}, \quad (3)$$

where c and h denote the cold and hot species, respectively. The Electron Acoustic dispersion relation is

$$\omega = \left(\omega_c^2 \frac{1 + 3(k\lambda_c)^2}{1 + (k\lambda_h)^{-2}} \right)^{\frac{1}{2}}. \quad (4)$$

Lastly the beam driven dispersion relation is simply

$$\omega = k u_d, \quad (5)$$

when the relative velocity of the beam is significantly large, u_d being the streaming velocity of the beam electrons.

3 Procedure

We use the same 1-D model with periodic boundary conditions described by Koen et al. with 1024 grid points, a grid spacing λ_c (the cold electron Debye length), and a time step of $0.1\omega_p^{-1}$ the plasma frequency calculated using the total electron density. The general iteration as described by Birdsall&Langdon and used in our code is as follows.

- On initialization the particle velocities are distributed following a Maxwellian distribution with velocities normalized to the cold electron velocity.
- The charge density is calculated by accumulating and weighted charges to their closest grid points.
- We then solve Poisson's Eq in frequency space by applying the FFT to the charge density, to find the potential and electric field.
- Then we update the particle positions and velocities using the new fields.

3.1 Initialization

Each species is initialized by a specified streaming speed and temperature, which determines the FWHM of the velocity distribution. Only the Beam electrons are initialized with a nonzero streaming speed. Lastly, since the velocity is normalized to the thermal speed of the cold electrons the temperatures of other species are specified in units of cold electron temperature.

3.2 Charge Density and Field Weighting

There are two methods for charge density weighting and field to particle interpolation, which determine the variety of conserved quantities in the simulation. This code utilizes the Energy conserving method described by Birdsall&Langdon although Koen et. al. does not specify whether the energy or momentum conserving methods were used. The energy conserving method treats charges as triangular distributions, allotting a fractional charge to the two closest grid points. The force on each particle, however, is determined purely by the electric field at the closest grid point.

3.3 Solving Poisson's Eq.

Since this code uses periodic boundary conditions it yields itself naturally to Fourier Transforms and Fourier space. We use a 1024-point FFT to calculate $\rho(k)$, which allows us to rewrite Poisson's equation as

$$\nabla^2 \phi(k) = \frac{\partial^2 \phi(k)}{\partial x^2} \quad \text{In one dimension} \quad (6)$$

$$k^2 \phi(k) = \frac{\rho}{\epsilon_0} \quad (6)$$

$$\phi(k) = \frac{\rho}{k^2 \epsilon_0} \quad [3] \quad (7)$$

We also set $\rho(k=0) := 0$ to ensure there is a net zero charge, this is how we implement the immobile background ions.

We then use the inverse Fast Fourier Transform algorithm to obtain the potential at the grid points, from which we arrive at the electric field by a gradient operator. The gradient operator is approximated using a derivative operator with periodic boundary conditions

$$\nabla \simeq \begin{pmatrix} 0 & 1 & 0 & \cdots & -1 \\ -1 & 0 & 1 & \cdots & 0 \\ \vdots & & \ddots & & \vdots \\ 0 & \cdots & -1 & 0 & 1 \\ 1 & 0 & \cdots & -1 & 0 \end{pmatrix} \in \mathbb{R}^{1024 \times 1024}. \quad (8)$$

$$\rho(x) \xrightarrow{\mathcal{FFT}} \rho(k) \xrightarrow{\frac{1}{k^2}} \phi(k) \xrightarrow{\mathcal{IFFT}} \phi(x) \xrightarrow{\nabla} E(x)$$

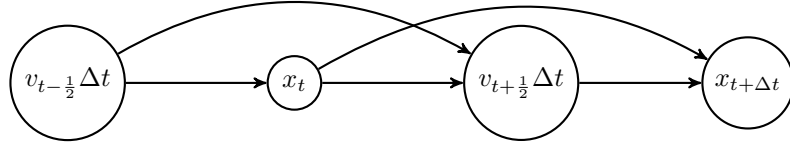
3.4 Equations of Motion

Finally the equations of motion are discretized as

$$\frac{v_i^{j+1} - v_i^j}{\Delta t} = \frac{q}{m} E_{nearest} \quad (9)$$

$$\frac{x_i^{k+1} - x_i^k}{\Delta t} = v_i^j. \quad (10)$$

The equations are solved using the leapfrog scheme. Velocities are updated at half time steps while positions are updated on full time steps.



Importantly, the first time step we set the velocities back a half time step by updating the fields using a charge of $-e/2$. The rotation that would be induced by the presence of a magnetic field is also ignored in this plasma since it is considered unmagnetized.

3.5 Parameters

Table 1 presents a summary of the parameters used in each of the runs which are exactly the same as those used by Koen et. al.

Table 1: Parameters for the simulation runs, matching those from Koen et. al.

Run	n_b/n_c	T_h/T_c	u_d/v_{Tc}
1	0.04	100	20
2	0.04	100	15
3	0.04	100	8
4	0.04	10	20
5	0.04	1	20
6	0.02	100	20
7	0.1	100	20

3.6 Dispersion Relations

Lastly, the Experimental dispersion relations were calculated by creating a history of the electric field, space and time. Koen et al. uses a temporal domain of $\approx 100 \omega_p$, which is approximately 1000 time steps using our time step. The 2-D FFT of this array, the electric field history over the past 1000 time steps, is then taken to find the experimental dispersion relations.

4 Results & Discussion

The difference in the simulations conducted by Koen et al. and ours is the time step and particle number. We use 2×10^5 particles and $0.1\omega_p^{-1}$ compared to the original 2×10^6 and $0.01\omega_p^{-1}$. Figure 1 shows the kinetic and potential energy of Run 1 over a timescale of $1500\omega_p$. Both the kinetic and electrostatic energy peaks at $50\omega_p$ and stabilizes at roughly $1000\omega_p$. These results agree with the findings in Koen et al. The kinetic energy values differ by a factor of roughly 10 which is inline with the difference in particle number. The discrepancy in the value of the potential energy peak was larger, roughly a factor of 6, which can be explained by the differences in electric field in the growth stage, the stabilization value, however, is about 4×10^3 which also agrees up to the difference in particle number.

Figure 2 shows the spatial profiles of the electric field for $t = 50\omega_p, 500\omega_p$, when compared with the electric field from Koen et al. our electric field is noticeably more noisy. This appears to be a consequence of the smaller electron number density, see Figure 3 for a comparison to a run with only 102 grid points. The number density is inversely proportional to the Debye length. Since the Debye length is characteristic distance needed to shield electric fields a larger Debye length could certainly explain this excess noise, although the grid spacing is determined by the Debye length the smaller number of particles will create more statistical fluctuations. Figure 3 shows that a smaller number of grid points does create a smoother E-field. However, the resulting 2-D FFT is near unusable due to degraded spatial resolution, see Figure 4. The electric field amplitude is also roughly a factor of 10 smaller. Other information is also less accurate such as the time of energy peaks and stabilization, Figure 8.

Another key difference is the lack of the bipolar structure noted by Koen et al. this is likely due to the fact larger time step not allowing the survival of the potential holes. Although in the original study the potential holes do also merge the holes in our simulations merge much earlier, around $400\omega_p$, see Figure 6.

Figure 5 shows the phase space diagrams of our plasma for $t = 50\omega_p$ and $t = 500\omega_p$. The behavior agrees with those demonstrated by Koen et al. in the formation of potential holes and heating of cold electrons, however as previously mentioned the potential holes do not survive to $t = 500\omega_p$.

Figure 7 shows the dispersion relations for Runs 1-7. Firstly, the resolution is much coarser due to the larger time step and lower number density of electrons. Taking these factors into mind, the results from Run 1 agree for the electron plasma and electron acoustic waves, although the beam driven wave mode seems to be more strongly damped.

Runs 2 and 3 investigate the effect of streaming speed. In Run 2, our simulations show the electron acoustic wave mode to be more damped than Run 1, which is the exact opposite of what was found by Koen et al. We did find that reducing the streaming speed of the beam electrons below the thermal velocity of the hot electrons keeps beam driven waves from forming, but there was not an appreciable beam driven wave in Run 1 to begin with. However, similar to Koen et al.'s results the plasma and acoustic waves are dominant in Run 3.

Runs 4 and 5 differ from the reference, Run 1, by beam temperature. There is no significant difference in the dispersion relations for $T_h/T_b = 10$ versus $T_h/T_b = 1$, however both have weaker acoustic wave modes which agrees with the theoretical prediction [1].

Runs 6 and 7 change the number of beam particles from the reference case. We expect to find stronger beam driven wave modes as compared with acoustic or plasma waves. However, Figure 7 shows that all waves modes are weaker in Runs 6 and 7 as compared to Run 1.

5 Conclusion

To summarize our results, we were able to accurately reproduce the plasma's electrostatic and kinetic energy and record the energy peaking and stabilizing at similar times. We reproduced the phase space diagrams of the Plasma for small time values, $< 200\omega_p$, where we observed similar potential holes. We were also able to record all three plasma wave modes.

However, we were not able to accurately recreate the Electric field profiles, our field was much noisier, caused by the decrease in number density. We found that reducing the number of grid points did remedy this, however, it also made the dispersion relation graphs inherently less informative due to the lack of resolution. Finally, we were not able to note the marked differences in wave modes due to the change of simulation parameters as noted by Koen et al. While our simulations revealed some accurate information, the original choice of particle and time step seems to be well justified in this case.

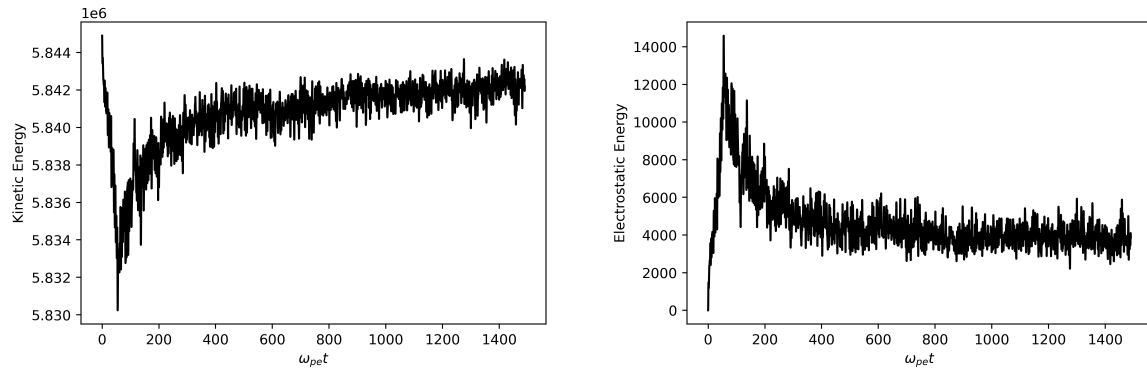


Figure 1: The evolution of the total Kinetic and Electrostatic Energy through time of Run 1.

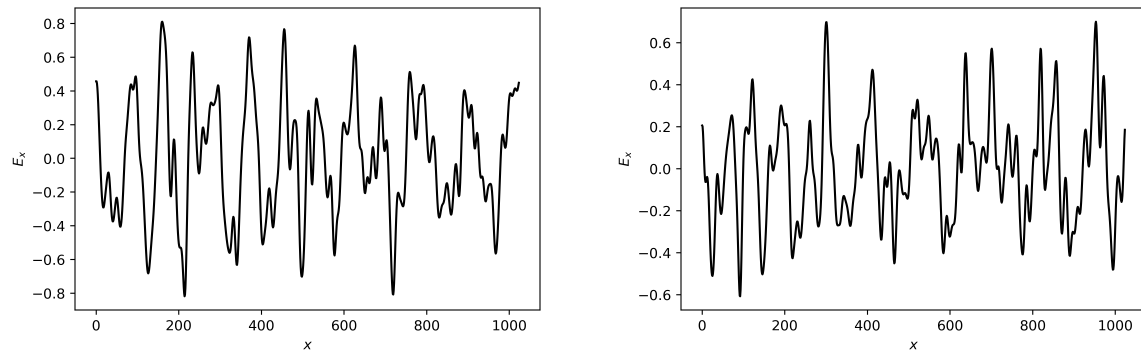


Figure 2: The spatial profiles of the electric field at $t = 50 \omega_p$ (left) and $t = 500 \omega_p$ (right).

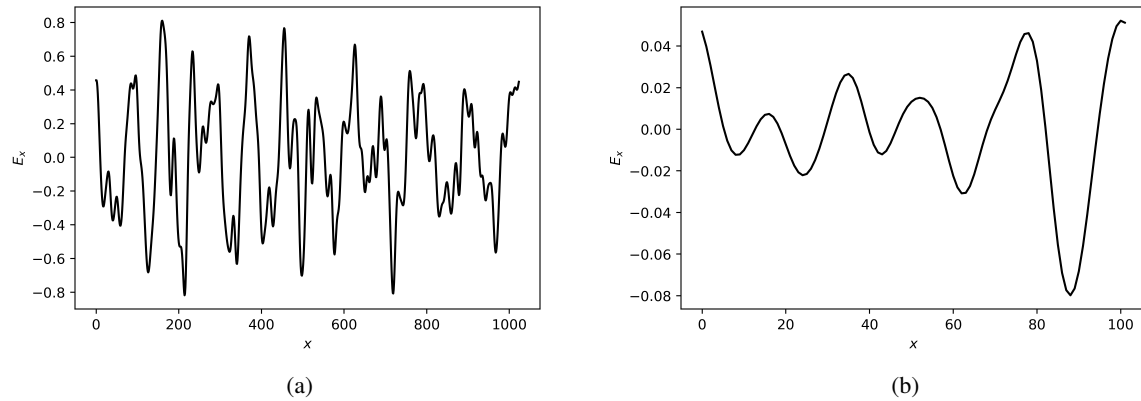


Figure 3: Spatial profiles of electric fields for Run 1 with 1024 grid points (a) and 102 grid points (b), both at $t = 50 \omega_p$.

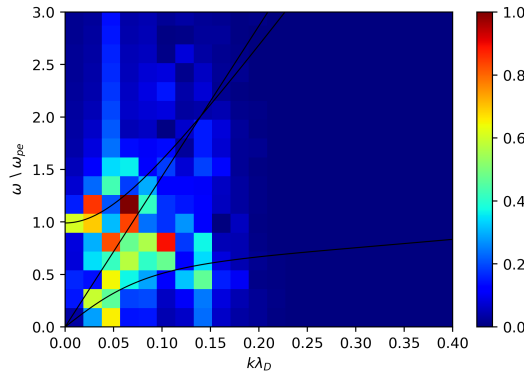


Figure 4: Dispersion relation for Run 1 with 102 grid points from $1200 \omega_p - 1302.4 \omega_p$.

6 Code

The code for this project can be accessed here
https://github.com/PhilipKlaass/305_final

References

- [1] Etienne J. Koen, Andrew B. Collier, and Shimul K. Maharaj. Particle-in-cell simulations of beam-driven electrostatic waves in a plasma. *Physics of Plasmas*, 19(4):042101, April 2012. _eprint: https://pubs.aip.org/aip/pop/article-pdf/doi/10.1063/1.3695402/13641152/042101_1_online.pdf.
- [2] S. Peter Gary and Robert L. Tokar. The electron-acoustic mode. *The Physics of Fluids*, 28(8):2439–2441, 08 1985.
- [3] Langdon A.B. Birdsall, C.K. Plasma physics via computer simulation (1st ed.). *CRC Press*, 1991.

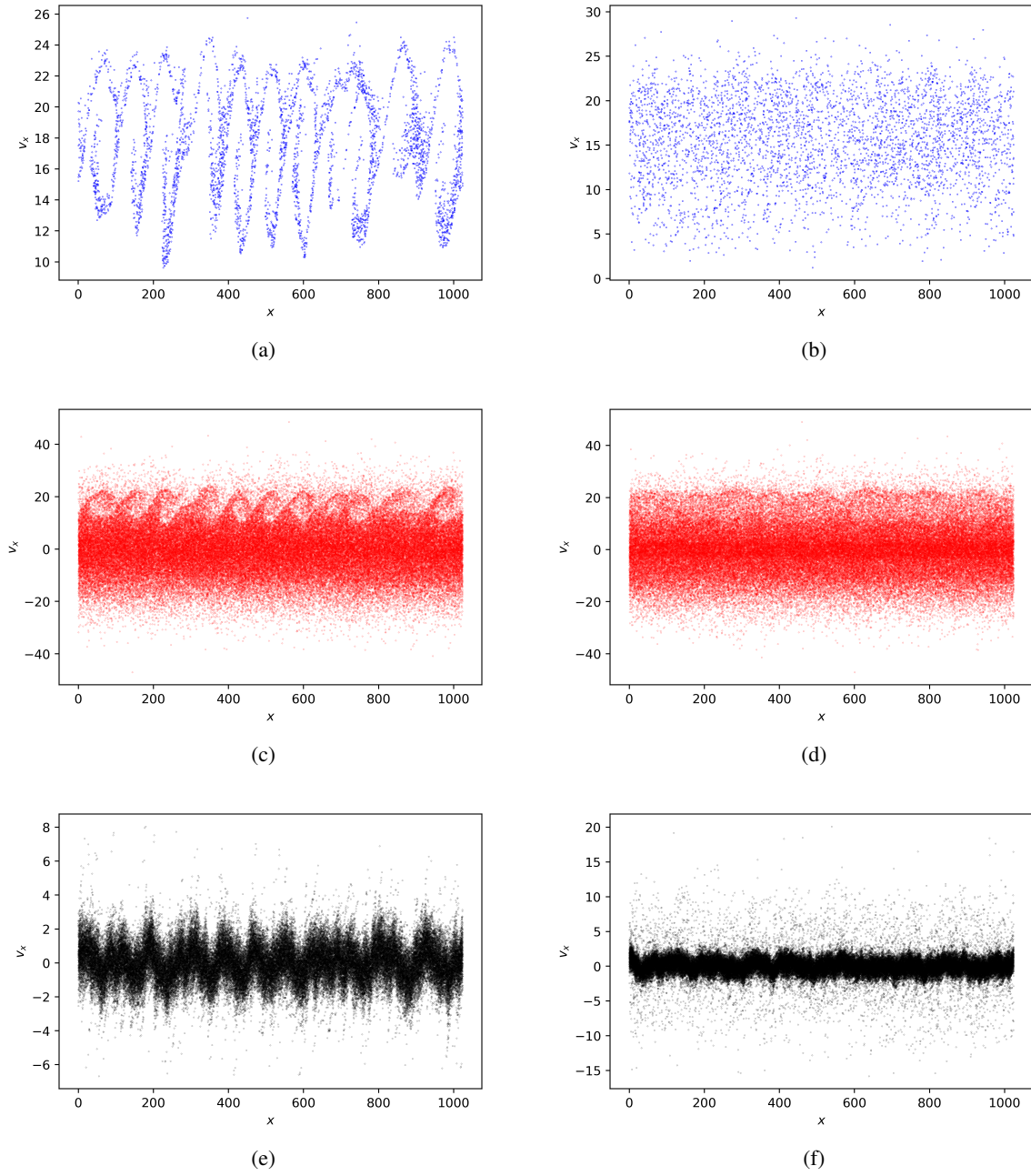


Figure 5: The three species, beam, hot, and cold in blue, red, and black respectively; at $t = 50 \omega_p$ on the left and $t = 500 \omega_p$ on the right

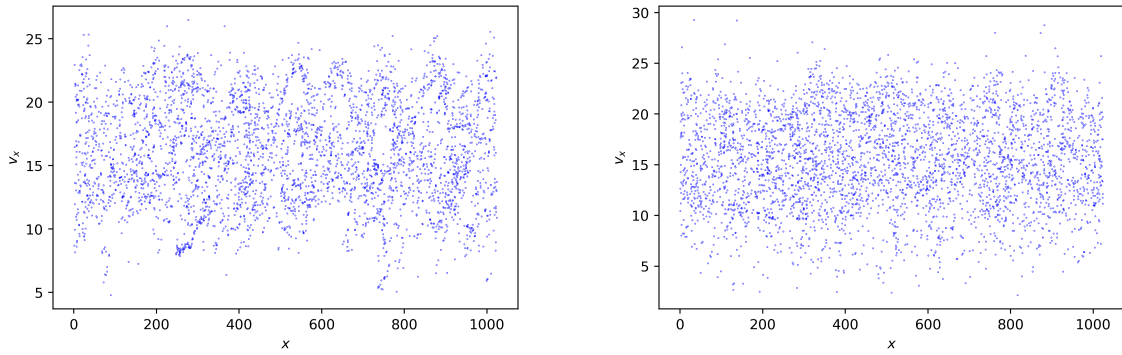


Figure 6: Potential holes can be seen on the left at $180 \omega_p$, around $x = 600$ and $x = 750$. However they have merged by $340 \omega_p$ on the right.

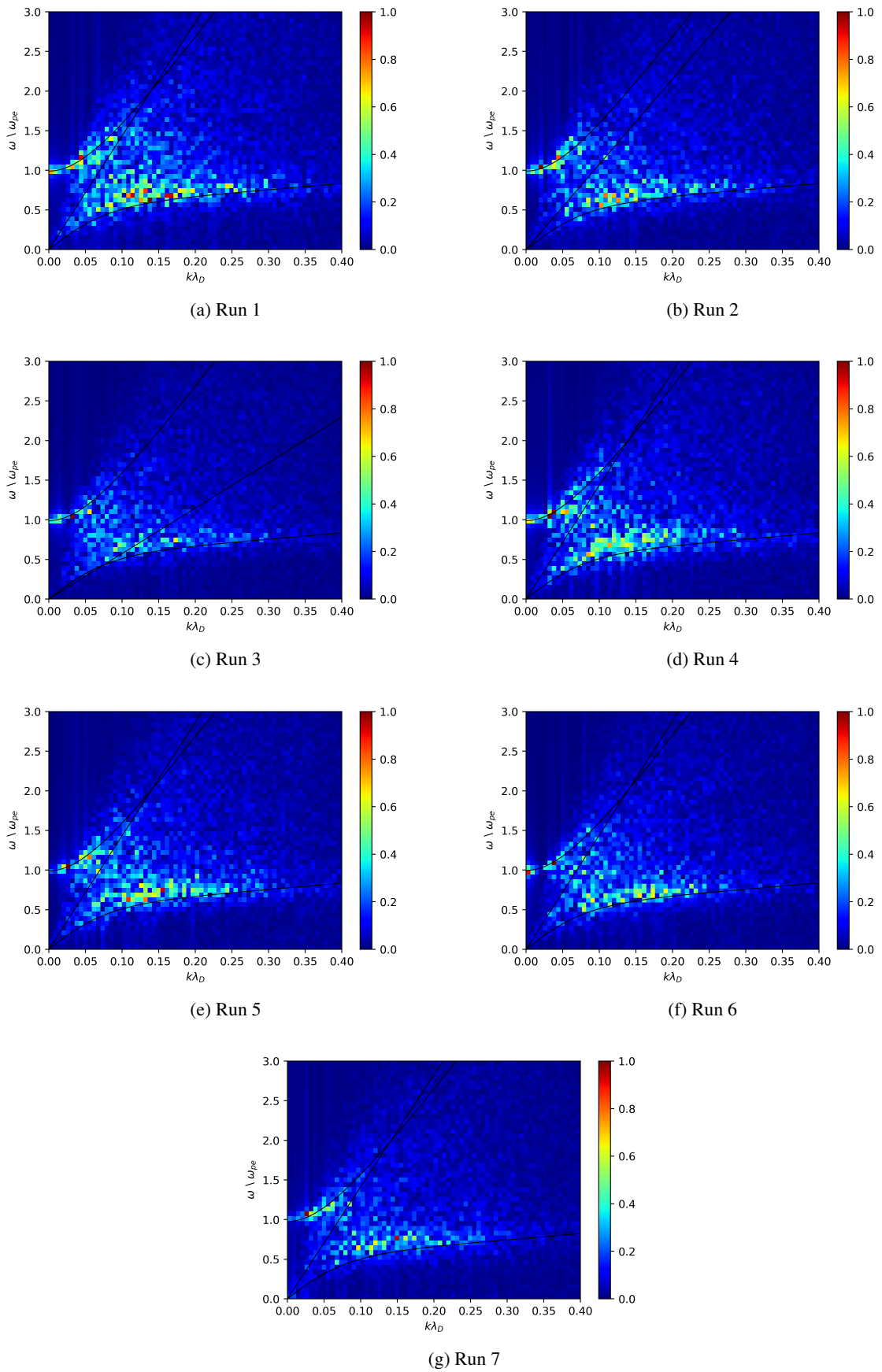


Figure 7: Dispersion relations for all 7 runs; 2-D FFT⁹ of the electric field history from $1200 \omega_p$ - $1302.4 \omega_p$

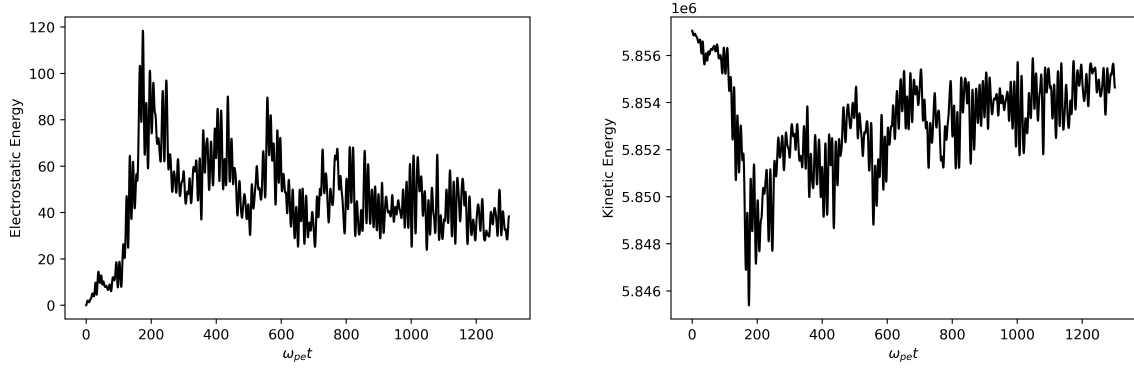


Figure 8: Potential and Kinetic energies for Run 1 with 102 grid points.